Magnetic light-matter interaction in a photonic nanocavity

M. Burresi,[1,*] T. Kampfrath,[1] D. van Oosten,[1] J. C. Prangsma,[1] B.-S. Song,[2,3] S. Noda,[2] and L. Kuipers[1]

[1] *Center for Nanophotonics, FOM Institute for Atomic and Molecular Physics (AMOLF), Science Park 104, 1098 XG Amsterdam, The Netherlands*

[2] *Department of Electronic Science and Engineering, Kyoto University, Kyotodaigaku-Katsura, Nishikyo-ku, Kyoto 615-8510, Japan.*

[3] *School of Information and Communication, Sungkyunkwan University, S Janan-Gu, Suwon 440-746, Korea.*

We study the influence of the proximity of a metal-coated dielectric aperture probe on the transmission of a sidecoupled photonic crystal nanocavity. We find that the resonance of the nanocavity shifts to shorter wavelengths when the ring-like apex of the probe is above an anti-node of the magnetic field of the cavity. We show that this can be attributed to Lenz' law. We use these measurements to determine the magnetic polarizibility of the apex of the probe and find good correspondence with theory. We discuss how this method could be applied to study the electric and magnetic polarizibilities of nano-objects.

PACS numbers:

Photonic crystals are materials which provide a high degree of control of the propagation of light at the nanoscale[**?**]. The most striking examples are photonic crystal nanocavities, that can trap light in volumes comparable to the cubed wavelength for many optical cycles[**? ?**]. Such nanocavities currently have only modestly narrow linewidths compared to their macroscopic counterparts, that have been used to detect and trap single atoms[**?**]. However, as the mode volume of photonic crystal nanocavities is typically upto 5 orders of magnitude smaller than that of a traditional high finesse cavity, one can still obtain a much higher sensitivity when studying the interaction of light with nano-objects. This sensitivity was exploited to tune the cavity resonance by bringing a small dielectric object into the cavity field[**? ?**]. Recently this effect was even used to control the emission spectrum photonic crystal nanolaser[**?**]. Up to now, these investigations have focused on the coupling between matter and the electric component of light, as the material response to magnetic fields is usually negligible at frequencies above a few THz. Recently, materials have been developed that exploit their geometry to induce a magnetic response at optical frequencies. The most well known examples of such materials are split-ring resonators[**?**]. The principles used in these so-called magnetic metamaterials have also been employed to measure the magnetic field of light at optical frequencies[**?**]. Given this interest in the magnetic properties of materials at optical frequencies, a means to measure these properties directly is desireably. A photonic crystal nano-cavity is perfectly suited for such studies, as the anti-nodes of the magnetic field inside the nanoresonator occur at the nodes of the electric field. This means the magnetic and electric response can be seperately determined by measuring how the response of the cavity to the proximity of an object depends on whether the object is above an anti-node in the magnetic or the electric field, respectively. This technique could make it possible to measure magnetic polarizibilities of any nano-object, such as split-ring resonators, quantum rings, carbon nanotubes or aromatic molecules, which are all subject of study because of their magnetic properties.

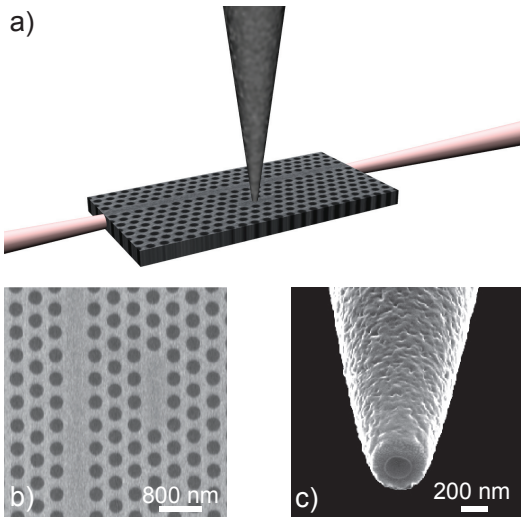

FIG. 1: (a) Schematic of the experiment. Light is loaded into a photonic-crystal nanocavity via a side-coupled photonic-crystal waveguide. An adjacent nanotip is used to both perturb the cavity and to scan the light distribution in and around the cavity. (b) Scanning electron micrograph of the photonic crystal nanocavity and access waveguide. (c) Scanning electron micrograph of the aperture probe, which consists of a silica core coated by aluminum.

In this work, we study how the resonance frequency of a photonic crystal nano-cavity shifts when we bring a near-field aperture probe in close proximity of the surface of the cavity. We observe that when the ring-like aperture of the probe is above an anti-node of the magnetic field, the cavity resonance shifts to shorter wavelengths. From this pronounced blue shift, we determine the magnetic polarizibility of the near-field aperture and find excellent

agreement with theory. Based on this result, we discuss the feasibility of using this method to measure the magnetic polarizibility of even smaller nano-objects.

The essential parts of our experiment are a nano-cavity and the perturbing tip, as shown in the schematic of Fig. 1(a). The nano-cavity can be pictured as a point-like defect in a photonic crystal, which is a periodically perforated 200 nm thick Si membrane [Fig. 1(b)]. The cavity is side-coupled to a photonic-crystal waveguide which is a missing row of holes separated from the cavity by three rows of holes. The resonance of the unperturbed cavity lies at a vacuum wavelength of $\lambda_{r0} = 1534.6\,\mathrm{nm}$ and exhibits a quality factor of $Q_0 = 6500$. We excite the cavity by coupling light of wavelength λ from a continuous-wave diode laser into the access waveguide. In order to perturb the cavity light field, an Al-coated dielectric tip is placed in the evanescent field tail at a constant height of 20 nm above the cavity surface [Fig. 1(a)]. The tip consists of a tapered single-mode optical fibre coated by a 100-nm thick Al film resulting in a highly cylindrical aperture with a diameter of 200 nm [Fig. 1(c)]. In order to characterize the interaction between tip and cavity, we detect the light at the other end of the access waveguide by means of a lensed fiber. By raster scanning the tip over the cavity surface, the waveguide transmittance $T(x, y, \lambda)$ as a function of in-plane tip position (x, y) and light vacuum wavelength λ is obtained. We also use the tip as a near-field probe and collect the minute fraction of light that enters the fiber through the tip aperture. By using an interferometric scheme, this allows us to map the complex-valued in-plane electric-field distribution of the light directly above the cavity surface.

Figure 2(a) displays the component $\mathrm{Re}\, E_y(x, y, \lambda)$ of the cavity field as obtained by a typical near-field measurement at resonance $\lambda = \lambda_{r0}$. The spatial structure of this image is in excellent agreement with that of the unperturbed cavity field as calculated by a finite-difference time-domain (FDTD) approach [Fig. 2(b)]. This agreement attests to the high quality of our near-field probe.

Next, Fig. 3(a) displays a map of the normalized waveguide transmittance $F(x, y, \lambda) = T(x, y, \lambda)/T_0(\lambda)$ acquired at resonance, $\lambda = \lambda_{r0}$. Here, T_0 is the waveguide transmittance in the absence of the tip. In the black regions of Fig. 3(a), the transmittance remains unchanged, whereas it has decreased in the blue regions and decreased in the yellow regions. To understand why this happens, Fig. 3(b) shows the normalized transmittance spectrum $F(x_1, y_1, \lambda)$ for the tip position indicated as 1 in Fig. 3(a). We see that for wavelengths around the unperturbed resonance at λ_{r0}, the transmittance increases. On the other hand, a dip of decreased transmittance is found at about $0.xx\,\mathrm{nm}$ below λ_{r0}. This observation is a clear hallmark of a tip-induced shift $\lambda_{r0} \rightarrow \lambda_r(x, y)$ of the cavity resonance: as the resonance wavelength shifts away from the laser wavelength, there is less coupling from the waveguide to the cavity. Less coupling,

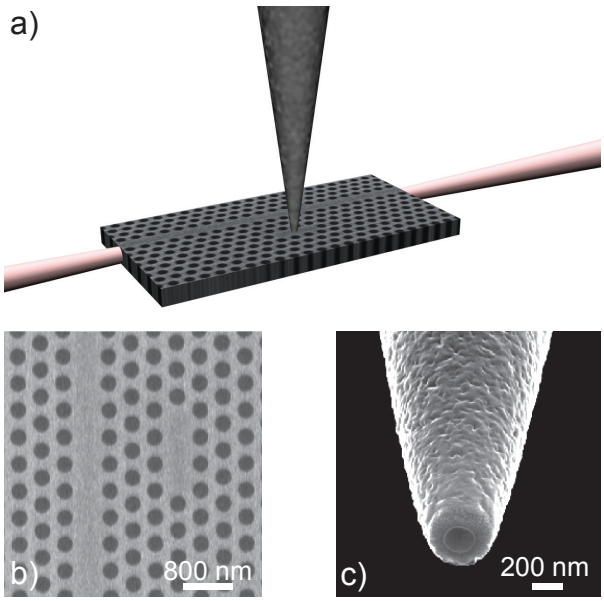

FIG. 2: Electric-field distribution in and around the cavity at resonance wavelength λ_{r0} as (a) measured with the tip (b) calculated by an FDTD approach.

in turn, reduces the overall losses the light experiences in the waveguide-cavity system and, thus, increases the waveguide transmittance at λ_{r0}. On the other hand, at the new resonance wavelength λ_r, the waveguide-cavity coupling has increased, which implies larger losses and reduced transmittance. In other words, the peak and the dip of F in Fig. 3(b) roughly indicate the resonance of the unperturbed and perturbed cavity, respectively. Qualitatively similar behavior is also found at other tip positions $2 \ldots 5$, as seen in Fig. 3(c).

We apply coupled-mode theory to our measured transmittance data F, which allows us to quantitatively extract the tip-induced resonance shift $\Delta\lambda_r = \lambda_r - \lambda_{r0}$ and a possible change in the quality factor. When the waveguide and the cavity are treated as coupled elements, the waveguide transmittance is given by [**?** **?**]

$$T(x, y, \lambda) = 1 - \frac{1/Q_v^2 - 1/Q^2}{4(\lambda_r/\lambda - 1)^2 + 1/Q^2}. \qquad (1)$$

The total quality factor Q is $1/Q = 1/Q_{in} + 1/Q_v$, where $1/Q_{in}$ and $1/Q_v$ quantify the cavity losses to the in-plane waveguide and the losses to free space in the vertical direction, respectively. Applying these relations to both the perturbed and the unperturbed cavity yields an expression $T(x, y, \lambda)/T_0(\lambda)$ which is fitted to the measured normalized transmission spectrum $F(x, y, \lambda)$ for each tip position (x, y). The position-dependent fit parameters are λ_r, Q_{in}, and Q_v whereas the values of λ_{r0}, Q_{in0}, and Q_{v0} are fixed. The resulting fits are in excellent agreement with the measured data as demonstrated by the red line in Fig. 3(b).

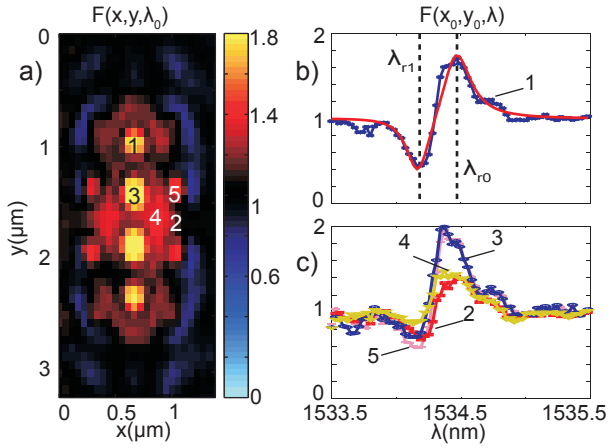

FIG. 3: (a) In-plane map of the normalized waveguide transmittance $F(x, y, \lambda_{r0})$ at the unperturbed cavity resonance. Black regions indicate unchanged transmission. (b) Normalized transmittance spectrum $F(x, y, \lambda)$ at probe position 1 in (a). The peak ($F > 1$) indicates the resonance of the unperturbed cavity whereas the dip ($F < 1$) arises from the new cavity resonance brought about by the presence of the tip. A fit (red solid line) to the spectrum allows us to extract the tip-induced shift of the resonance. (c) Same as (b) for probe positions 2 . . . 5 in (a).

The extracted relative shift $\Delta\lambda_r/\lambda_{r0}$ of the cavity resonance is displayed in Fig. 4(a) as a function of tip position. This map is consistent with the raw data $F(x, y, \lambda_{r0})$ in terms of the spatial structure [Fig. 3(a)] and in terms of the magnitude of the resonance shift: as suggested by Fig. 3(b), a blue-shift of up to 0.45 nm is found at certain tip positions. It is highly instructive to compare the map of $\Delta\lambda_r/\lambda_{r0}$ of Fig. 4(a) to Figs. 4(b) and (c) which, respectively, show the modulus $|B_{z0}|$ of the out-of-plane magnetic component and the modulus $|\boldsymbol{E}_0|$ of the total electric component of the unperturbed cavity field as calculated by a finite-difference time-domain approach. Surprisingly, the spatial symmetry of the $\Delta\lambda_r/\lambda_{r0}$ image closely and exclusively resembles that of $|B_{z0}(x, y, \lambda_{r0})|$. On the other hand, no features of the symmetry of $|\boldsymbol{E}_0(x, y, \lambda_{r0})|$ are discernible. We conclude that the cavity-tip interaction is dominated by the magnetic rather than the electric component of the cavity light field.

This observation becomes plausible when we consider the tip as a metallic ring the thickness of which is given by the 100 nm long evanescent tail of the cavity light field. According to Faraday's law, the magnetic-field component B_z induces a circular current in the ring-like tip apex. As described by Lenz' law, this current generates a magnetic field that opposes and, thus, reduces the driving field. As a consequence, the effective cavity volume shrinks, leading to a resonance shift towards higher frequencies and shorter wavelengths. In other words, the observed blue-shift of the cavity resonance can be understood as a direct manifestation of Lenz' law at the nanoscale. Our finding is in sharp contrast to previous work which all reported a red-shift [**?** **?**]. In these experiments, dielectric or metallic tips with dimensions much smaller than the wavelength and the penetration depth of the light were used. In this situation, the field energy inside the tip is increased, which increases the effective cavity mode volume, implying a red-shift of the resonance [**?** **?**].

To put this discussion on a more quantitative basis, we note that the induced relative resonance shift of the cavity is given through perturbation theory [**?**] by

$$\frac{\Delta\lambda_r}{\lambda_{r0}} = \frac{\Delta U}{U_0}. \tag{2}$$

Here, $U_0 = (2/\mu_0)\int \mathrm{d}^3\boldsymbol{x}\,|\boldsymbol{B}_0(\boldsymbol{x})|^2$ is the energy of the unperturbed cavity field, and $\Delta U = (\lambda_{r0}/2\pi ic)\int \mathrm{d}^3\boldsymbol{x}\,\boldsymbol{j}^*\cdot\boldsymbol{E}_0$ is its tip-induced change which arises from the induced current density $\boldsymbol{j}$ in the tip. ΔU can also be understood as the work done when the tip adiabatically approaches the loaded cavity. In the dipole approximation, ΔU equals $\boldsymbol{E}_0^*\cdot\boldsymbol{p}+\boldsymbol{B}_0^*\cdot\boldsymbol{m}$, where the induced electric and magnetic dipole moments $\boldsymbol{p} = \alpha^{\mathrm{ee}}\boldsymbol{E}_0$ and $\boldsymbol{m} = \alpha^{\mathrm{mm}}\boldsymbol{B}_0$ are connected to the fields through the electric and magnetic polarizability α^{ee} and α^{mm}, respectively. Because of the cylindrical symmetry of the tip, there is no cross-coupling between electric and magnetic quantities, and the polarizability tensors are diagonal with $\alpha^{\mathrm{ee}}_{xx} = \alpha^{\mathrm{ee}}_{yy}$ and $\alpha^{\mathrm{mm}}_{xx} = \alpha^{\mathrm{mm}}_{yy}$. Since $|E_z| \ll |E_x|$ and ... ... exclude further elements... Eq. (2) turns into

$$\frac{\Delta\lambda_r}{\lambda_{r0}} = \alpha^{\mathrm{ee}}_{xx}\frac{|E^2_{0x}| + |E^2_{0y}|}{U_0} + \alpha^{\mathrm{mm}}_{zz}\frac{|B^2_{0z}|}{U_0}. \tag{3}$$

As suggested by Eq. (3) and the comparison of the maps of the measured resonance shift [Fig. 4(a)] and calculated fields [Figs. 4(b) and 4(c)], the tip response is dominated by $\mu_0\alpha^{\mathrm{mm}}_{zz}$. The observed blue-shift of the cavity resonance further implies that $\alpha^{\mathrm{mm}}_{zz}$ is negative. In order to extract values of α... from our experimental data, we compare the measured $\Delta\lambda_r/\lambda_{r0}$ to Eq. (3). As input, we use the FDTD calculated fields of the unperturbed cavity [Figs. 4(b) and 4(c)]. We choose the value of $\alpha^{\mathrm{mm}}_{zz}$ such that we obtain agreement with the measured resonance shift at tip position indicated as xxx in Fig. **??** where $|B_{0z}|$ is maximum and $|\boldsymbol{E}_0|$ vanishes. This procedure yields $\alpha^{\mathrm{mm}}_{zz} = 1\times10^{-22}\,\mathrm{m}^3/\mu_0$. **Now I want to estimate α_{ee}. I have not yet figured out how to precisely do and sell that.** On the other hand ee ... yields 0; however, error of measured $\Delta\lambda_r/\lambda_{r0}$ determines error of the polarizabilities, i.e.

Now the discussion of the αs. The value of $\mu_0\alpha^{\mathrm{mm}}_{zz}$ is reasonable as it is ... times the volume of the dielectric tip core. Estimates of $\mu_0\alpha^{\mathrm{mm}}_{zz}$ based on a quasistatic treatment yields ... which agrees well with the experimentally inferred value. The considerably smaller extracted magnitude of $\mu_0\alpha^{\mathrm{ee}}_{xx}$ may come as a surprise since

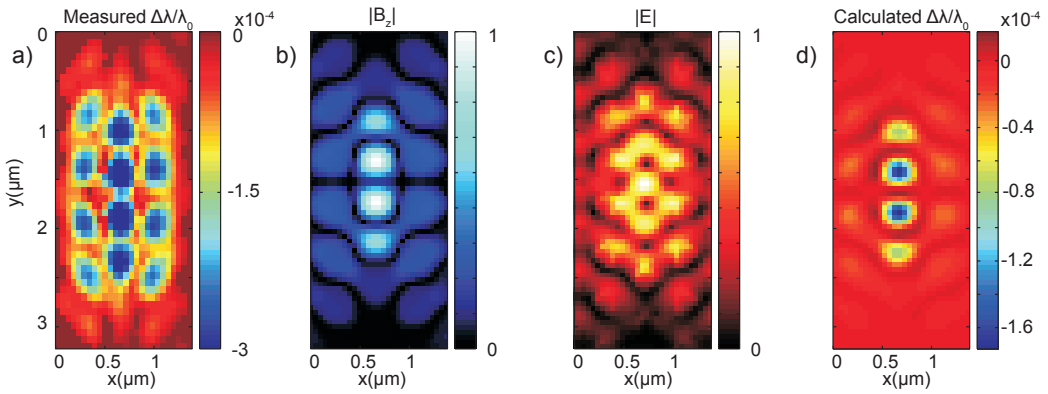

FIG. 4: (a) In-plane map of the relative shift of the resonance frequency of the cavity. (b) Modulus $|B_{z0}$ of the out-of-plane magnetic component of the light field in the symmetry plane of the unperturbed cavity at $\lambda = \lambda_{r0}$ as calculated by an FDTD approach. (c) Same as (b) for the modulus $|\boldsymbol{E_0}|$ of the total electric field. (d) Predicted relative shift in resonance frequency based on Eq. (**??**) and the FDTD-calculated field distributions.

the electric-dipole response is usually larger than the magnetic-dipole response. On the other hand, there are already simple geometric structures with sub-wavelength dimensions for which this statement is not true. First, a perfectly conducting sphere already shows a sizeable negative magnetic response, $\mu_0\alpha_{xx}^{\mathrm{mm}} = -\mu_0\alpha_{xx}^{\mathrm{ee}}/2 < 0$. Second, for an aperture in a perfectly conducting screen, the magnetic response is even twice as large as that of the negated electric response, $\mu_0\alpha_{xx}^{\mathrm{mm}} = -2\mu_0\alpha_{xx}^{\mathrm{ee}} < 0$ [**?**]. For a ring, which is the classical example of a structure with large inductance and, thus, magnetic polarizability, this trend can be expected to be even more pronounced. We finally note that a split-ring-type aperture already exhibits a cross-polarizability $\mu_0\alpha_{xy}^{\mathrm{me}}$ that exceeds the electric one by a factor of two.

To use this detection method for other nano-objects, we have to discuss the figure of merit for detection in this system. A polarizibility is easily detected if the shift $\delta\lambda$ of the cavity resonance is larger than the width $\Delta\lambda$. The cavity used in this work has a quality factor of 6500, which means it has a relative linewidth of $\Delta\lambda/\lambda_0 = 1/Q_0 \approx 1.5 \cdot 10^{-4}$. As the relative shift is $\delta\lambda/\lambda_0 \approx 4 \cdot 10^{-4}$, we can comfortably measure the magnetic polarizibility of our near-field probe with this configuration. Increasing the power into the waveguide does not improve the sensitivity, as it will increase both the work done by the nano-object and the unperturbed total energy of the cavity. However, we can increase the sensitivity of the system by choosing a cavity with a higher quality factor. As cavities with a quality factor $Q > 10^7$ have recently become available, it should be possible to detect relative shift of $\delta/\lambda = 1/Q \approx 10^{-7}$ and therefore to measure magnetic polarizations 3 orders of magnitude smaller than that of our probe, *i.e.* as long as $|\alpha^{\mathrm{mm}}| > 5 \cdot 10^{-24}\mathrm{m}^3/\mu_0$. For comparison, the near-resonant magnetic polarizibility of a two-level system such as an alkali atom is typically a few times $10^{-21}\mathrm{m}^3/\mu_0$ and that of a typical split-ring resonator has recently been shown to be around $2 \cdot 10^{-20}\mathrm{m}^3/\mu_0$. Thus, the method demonstrated here shows great promise to measure the magnetic and electric polarizibilities of many types of small objects ranging from single atoms and single molecules, all the way up to the nano scale.

In conclusion, we have shown how the resonance of a photonic crystal nanocavity is influenced by the proximity of a sub-wavelength sized metallic ring. Using coupled mode theory, we have extracted the resonance wavelength and quality factor from the data and observed that when the ring is above an anti-node of the magnetic field of light inside the cavity, the resonance of the nanocavity shifts to shorter wavelength. The observed shift is consistent with our estimates of the magnetic polarizibility of such a ring. Surprisingly, we find that the magnetic coupling between the cavity and the metallic nano-ring can increase the quality factor of the system by upto 50%. This effect will be further discussed in a forthcoming publication. Besides raising fundamental questions about the magnetic interaction between light and matter, our results demonstrate that photonic crystal nanocavity can be used to investigate the magnetic properties of specific nano-objects at optical frequencies. The development of magnetic metamaterials can greatly benefit from this characterization technique.

* Electronic address: burresi@amolf.nl

[1] To calculate the energy of the unperturbed cavity field, we assume that for the out-of-plane coordinates, the magnetic field is constant within the thickness d_{Si} of the Si membrane and that it decays exponentially into the surrounding air with a 1/e lentgh d_{air} of 100 nm. Then,

$U_0 = (2/\mu_0)(d_{\mathrm{Si}} + 2d_{\mathrm{air}}) \int\int \mathrm{d}x\mathrm{d}y\, |\boldsymbol{B}_0(x, y, 0)|^2$, where $\boldsymbol{B}_0(x, y, 0)$ is obtained from the FDTD calculations.